

Fracture behaviour of some rubber-toughened nylon 6 blends

Y. Kayano[†], H. Keskkula and D. R. Paul*

Department of Chemical Engineering and Center for Polymer Research,
 University of Texas at Austin, Austin, TX 78712, USA
 (Received 28 April 1997; revised 30 June 1997)

The high speed fracture characterization of various nylon 6/SEBS-*g*-MA and nylon 6/EPR-*g*-MA blends by the standard Izod impact test and the Vu-Khanh methodology is reported. This characterization provides a more in-depth examination of the influences of nylon 6 molecular weight and rubber types on fracture behaviour, expanding on a previous report that examined the standard Izod impact strength of nylon 6 blends with various maleic anhydride grafted styrene-(ethylene-*co*-butylene)-styrene (SEBS-*g*-MA) materials including the ductile–brittle transition behaviour that occurs when the rubber particle size and the test temperature are varied. Morphological features near crack tips formed at high speed were examined by microscopy to gain insight about the sequence of events that occur during crack propagation. This study has shown a linear relationship between toughness parameters *versus* the deformed zone size for all the blends. This suggests that the energy absorption for these rubber-toughened blends stems mainly from plastic deformation of the matrix which is induced by rubber cavitation. TEM observations of the region near the crack tip show that the extent of rubber particle cavitation depends on the nylon 6 matrix molecular weight. © 1998 Elsevier Science Ltd. All rights reserved.

(Keywords: nylon; SEBS; EPR)

INTRODUCTION

The toughening of polyamides with maleated elastomers such as ethylene–propylene rubber, EPR, or hydrogenated styrene/butadiene triblock copolymers, SEBS, has been of considerable commercial and scientific interest^{1–15}. A grafted copolymer is generated by reaction of the maleic anhydride grafted to the rubber, e.g., EPR-*g*-MA or SEBS-*g*-MA, and the amine end groups on the polyamide chain, which improves interfacial strength between the phases and the dispersion of the rubber particles in the polyamide matrix. The morphology of such blends is a key issue in the degree of toughening achieved and is influenced by a number of factors including the degree of maleation of the rubber, end group content and configuration of the polyamide, rheological characteristics, processing conditions etc.^{8,16–19}. The optimum range of rubber particle sizes has been interpreted in terms of a model that considers the interparticle distance, which leads to an upper limit of $\sim 1 \mu\text{m}$, and the difficulty in cavitation of small rubber particles, which leads to a lower limit of $\sim 0.1 \mu\text{m}$ ^{1,3,6,20–26}.

The standard notched Izod impact test or a similar procedure is commonly used to characterize the toughness of such blends. These procedures have been standard methods in the plastics industry because of their convenience, and allow easy comparison with other systems; however, the fracture energies obtained by these tests are certainly not material constants and provide only a limited picture of how the material responds to stress in the presence of a crack.

Understanding of fracture mechanics offers more sophisticated test methods to better characterize the toughness and to understand the deformation mechanisms that occur in toughened engineering thermoplastics^{27–43}. However, determination of the classical critical stress intensity factor (K_{IC}) based on linear elastic fracture mechanics (LEFM) requires testing of very thick specimens, which cannot be formed easily by injection moulding, of materials having low yield strength and high toughness, like rubber-toughened blends, in order to satisfy the small-scale yield criterion^{44,45}. The J -contour integral method has been recently regarded as more appropriate for such polymeric materials and alleviates to some degree this stringent thickness requirement^{45,46}; however, the thickness required is still often beyond what can be conveniently injection moulded. Rigorous measurement of J_{IC} involves use of rather specialized equipment and techniques.

A technique recently proposed by Vu-Khanh³⁶ offers an approach for characterizing fracture that is a useful compromise between rigorous fracture mechanics methodology and the simplicity of Izod or Charpy measurements. In this method, the energy required to fracture a specimen, U , with a ligament area, A , is measured by a standard or instrumented impact tester. It has the advantage of high test speeds corresponding to impact conditions as opposed to essentially static loading conditions usually employed in J_{IC} measurements. The analysis of this type of data, as proposed by Vu-Khanh, yields a fracture energy at initiation, G_i , and a measure of the additional energy associated with propagating the fracture, or tearing modulus, T_a . Vu-Khanh has claimed that the fracture energy at initiation, G_i , is equivalent to the critical J -integral for fracture, J_{IC} . Mai⁴⁷ pointed out that the Vu-Khanh approach is equivalent to the essential work analysis

* To whom correspondence should be addressed

[†] Permanent address: Mitsubishi Engineering-Plastics Corp., 6-2 Higashi-Yawata, 5-chome, Hiratsuka-shi 254, Japan

proposed by Mai, Williams and colleagues^{34,48–50} and have questioned equating G_I to J_{IC} . Regardless of the interpretation used, this approach provides considerable useful information about the fracture process that goes well beyond the Izod or Charpy tests, both of which may be regarded as single-point methods (one value of A) in this context.

Previous papers have examined the standard Izod impact strength of nylon 6 blends with various maleated elastomers, including the ductile–brittle transition behaviour that occurs when the rubber particle size and the test temperature are varied, and have shown that these quantities depend on polyamide molecular weight for fixed blend morphology^{11–15}. A subsequent paper examined the fracture behaviour of blends of varying rubber particle size using various toughness evaluation methods and *post mortem* transmission electron microscopy techniques⁵¹. The purpose of this paper is to provide more in-depth examination of the effect of rubber type and matrix molecular weight on the fracture behaviour of these blends, using the evaluation methods previously reported.

EXPERIMENTAL

Two commercial nylon 6 materials from Allied-Signal that differ only in molecular weight were used in this work; they are designated here by the prefixes L (for low) ($\bar{M}_n = 22\,000$) and H (for high) ($\bar{M}_n = 29\,300$) to denote their relative molecular weight. These materials were blended with various maleated and unmaleated styrene–ethylene/butylene–styrene triblock copolymers and a maleated ethylene–propylene copolymer to achieve

toughening; see *Table 1* for pertinent information. One of the block copolymers, designated by the prefix L, contains a relatively low content of styrene, which causes this material to have a lower modulus than the standard commercial SEBS materials in *Table 1*. Compositions of the blends prepared for this study are shown in *Table 2*.

Before melt processing, all the polymers were dried for 16 h at 80°C in a vacuum oven. A Killion single-screw extruder ($L/D = 30$, $D = 2.54$ cm) outfitted with an intensive mixing head on the screw was used for extrusion blending. Nylon 6/SEBS blends were extruded twice at 240°C and 40 rpm to ensure adequate mixing¹¹. A masterbatch process was used to prepare nylon 6/EPR-*g*-MA blends to obtain larger rubber particle sizes. A 50/50 nylon 6–EPR-*g*-MA mixture was made in the first step, after which this blend was diluted to an 80/20 ratio in a second step, both at 240°C and 40 rpm. The procedure for injection moulding these blends into test bars, either 3.13 mm or 6.25 mm thick, was the same as used in previous work⁵¹. Specimens without defects were selected for testing and kept in a desiccator under vacuum to avoid water sorption by the polyamide matrix^{52,53}.

An instrumented Dynatup Drop Tower Model 8200 was used for impact testing in addition to the standard Izod test. Specimens with standard notches or sharp notches were tested in the single-notch, three-point-bend configuration (SN3PB). All tests were made by dropping a 10 kg weight at a speed of 3.5 m s⁻¹, which is the same as that specified in the standard Izod test, using a span size of 48 mm. Details of the testing procedures are described elsewhere^{51,54}.

Transmission electron microscopy (TEM) was used to observe the deformation around the tip of arrested cracks.

Table 1 Materials used

Designation used here	Material (commercial designation)	Composition	Molecular weight	Source
L-Nylon 6	Nylon 6 (Capron 8207F)	End-group content: [NH ₂] = 47.9 μeq g ⁻¹ ; [COOH] = 43.0 μeq g ⁻¹	$\bar{M}_n = 22\,000$	Allied-Signal Inc.
H-Nylon 6	Nylon 6 (Capron 8209F)	End-group content: [NH ₂] = 34.8 μeq g ⁻¹ ; [COOH] = 28.8 μeq g ⁻¹	$\bar{M}_n = 29\,300$	Allied-Signal Inc.
SEBS	Styrene/ethylene–butene/styrene (Kraton G 1652)	29% styrene	Styrene block = 7000 EB block = 37 500	Shell Chemical Co.
SEBS- <i>g</i> -MA-2%	Styrene/ethylene–butene/styrene (Kraton FG-1901X)	29% styrene 1.84 wt% MA	—	Shell Chemical Co.
L-SEBS- <i>g</i> -MA	Styrene/ethylene–butene/styrene (RP-6509)	13% styrene 1.4 wt% MA	—	Shell Chemical Co.
EPR- <i>g</i> -MA	Exxelor 1803	43% ethylene 53% propylene 1.14 wt% MA	—	Exxon Chemical Co.

Table 2 Blend compositions

Designation used here	Composition	wt% MA in rubber
L-Nylon 6	100% 8207F	N/A
H-Nylon 6	100% 8209F	N/A
L-Nylon 6 + (25% SEBS- <i>g</i> -MA-2% + 75% SEBS)	80% 8207F + 20% (25% FG-1901X + 75% G-1652)	0.46%
L-Nylon 6 + L-SEBS- <i>g</i> -MA	80% 8207F + 20% RP6509	1.4%
H-Nylon 6 + L-SEBS- <i>g</i> -MA	80% 8209F + 20% RP6509	1.4%
L-Nylon 6 + EPR- <i>g</i> -MA	80% 8207F + 20% EPR- <i>g</i> -MA	1.1%

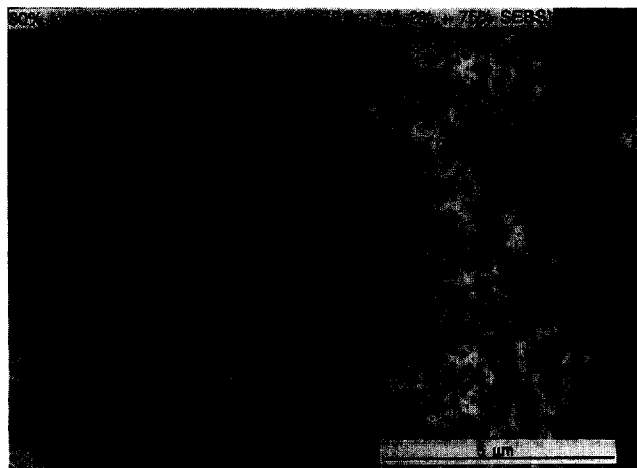


Figure 1 TEM photomicrograph of a blend of L-Nylon 6 with a rubber phase containing a 75% SEBS-g-MA-2% + 25% SEBS mixture; RuO₄ stained

These cracks were generated in 6.25 mm thick specimens with a 10 mm ligament size, using techniques described previously^{51,54}.

METHODOLOGY

Figure 1 shows the morphology of a blend of the lowest molecular weight nylon 6, designated here as L-Nylon 6,

containing 20% of a rubber phase, consisting of 25% of the maleated triblock copolymer SEBS-g-MA-2% and 75% of the unmaleated triblock copolymer SEBS, stained by exposure to the vapours of a ruthenium tetroxide solution (0.5%) for 20 min. Figures 2 and 3 show the morphology of blends of the highest and lowest molecular weight nylon 6 materials with the maleated triblock copolymer L-SEBS-g-MA stained by RuO₄, using the conditions mentioned above (Figure 2a and Figure 3a), and by phosphotungstic acid or PTA solution for 30 min at room temperature (Figure 2b and Figure 3b); RuO₄ stains the rubber phase dark whereas PTS stains the nylon phase dark. Samples stained by RuO₄ show the microdomain structure of the block copolymer phase. The morphology, using PTA staining, of L-Nylon/EPR-g-MA blends is shown in Figure 4. Photomicrographs of blends stained using PTA were employed for particle size analysis by a semi-automatic digital analysis technique based on Image® software from the National Institutes of Health. Weight-average particle diameters, \bar{d}_w , computed from these results are summarized in Table 3.

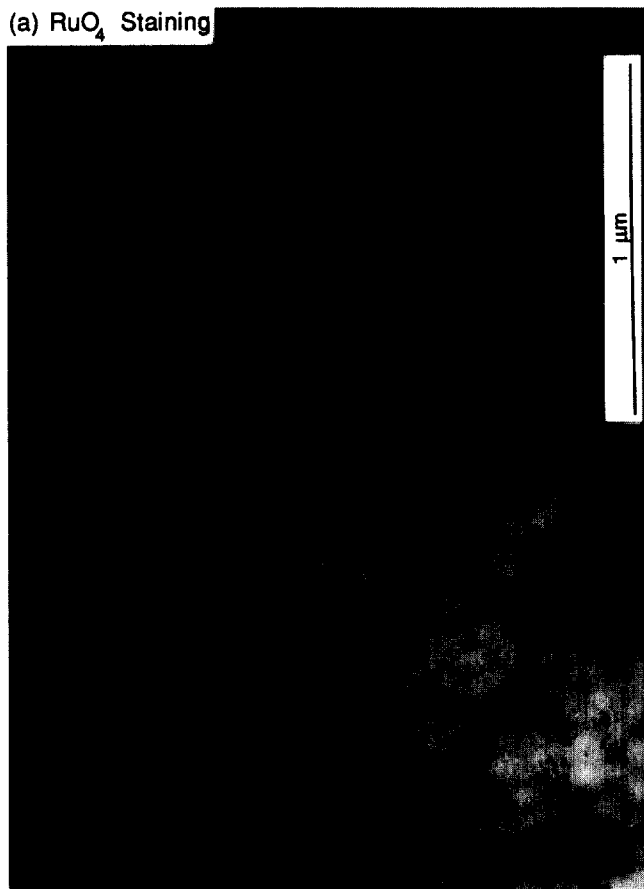
As shown previously¹⁴, the rubber particles in the blend based on the high molecular weight grade of nylon 6, H-Nylon 6, are slightly smaller than those in the blend based on the low molecular weight nylon 6, L-Nylon 6.

IZOD IMPACT STRENGTH AS A FUNCTION OF TEMPERATURE

Figure 5 shows the Izod impact strength as a function of

80% L-Nylon 6 (8207F) + 20% L-SEBS-g-MA

(a) RuO₄ Staining



(b) PTA Staining

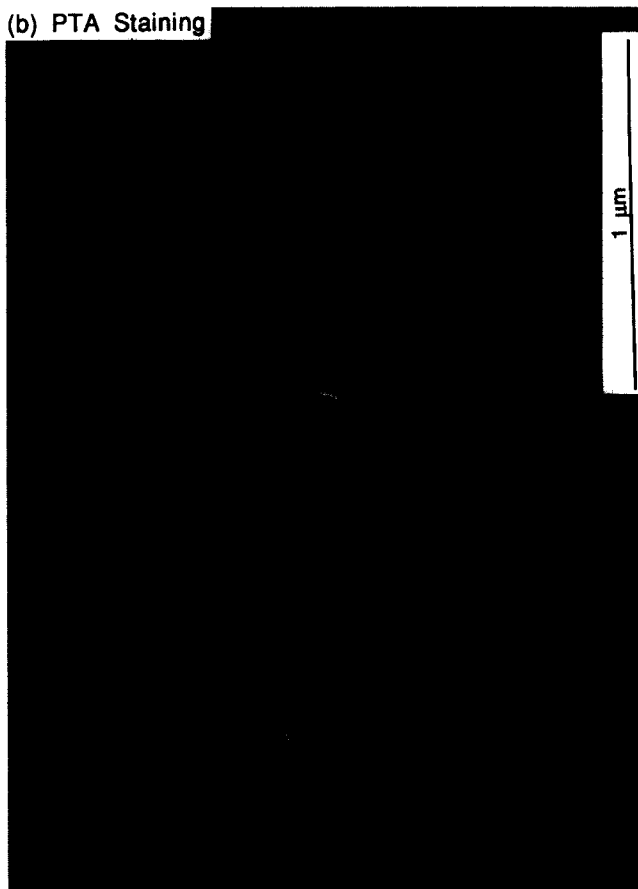


Figure 2 TEM photomicrographs of a blend of L-Nylon 6 with L-SEBS-g-MA: (a) RuO₄ stained; (b) PTA stained

80% H-Nylon 6 (8209F) + 20% L-SEBS-g-MA

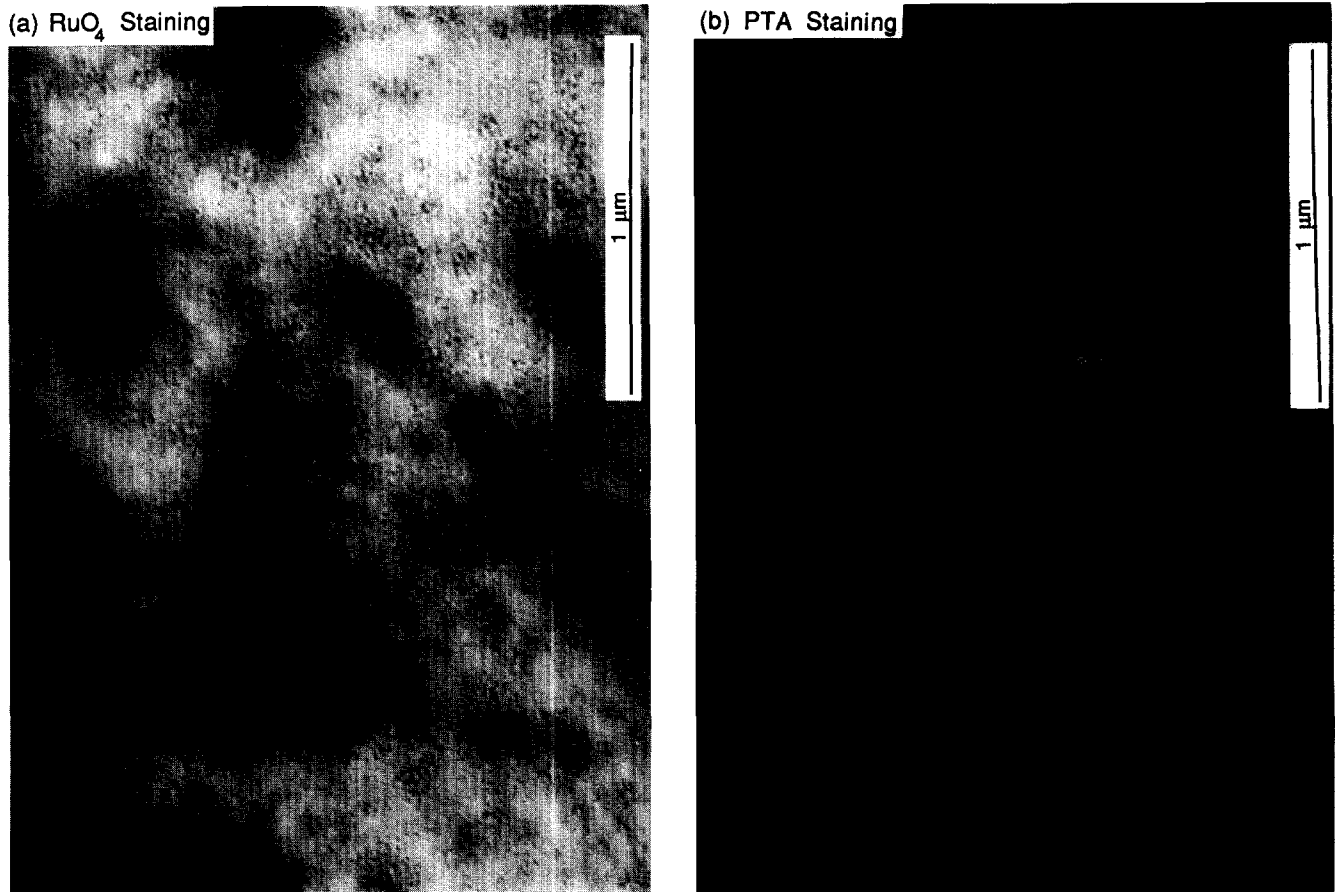


Figure 3 TEM photomicrographs of a blend of H-Nylon 6 with L-SEBS-g-MA: (a) RuO₄ stained; (b) PTA stained

testing temperature of thin (3.13 mm) specimens with standard notches for the various blends and pure polyamides listed in Table 2. The impact strength at room temperature and the ductile–brittle transition temperatures of these materials are summarized in Table 4. The neat polyamides, H-Nylon 6 and L-Nylon 6, have essentially the same impact strength and are brittle at all testing temperatures used. The blend based on 25% SEBS-g-MA-2%/75% SEBS shows the highest room temperature impact strength of all the blends in Table 2, while the L-Nylon 6/EPR-g-MA blend shows the

lowest ductile–brittle transition temperature, –40°C. The L-Nylon 6/EPR-g-MA and H-Nylon 6/L – SEBS-g-MA blends have the highest impact toughness at –20°C; however, both show some loss in toughness at higher testing temperatures. The former blend shows an increase in impact strength above room temperature. Figure 6 shows a plot of room temperature impact toughness as a function of the weight-average rubber particle diameter for each of these compositions, simply as a convenient method of summarizing these results. Because of the difference in polyamide molecular weight and the variation in the structures and properties of the rubber, a unique relationship

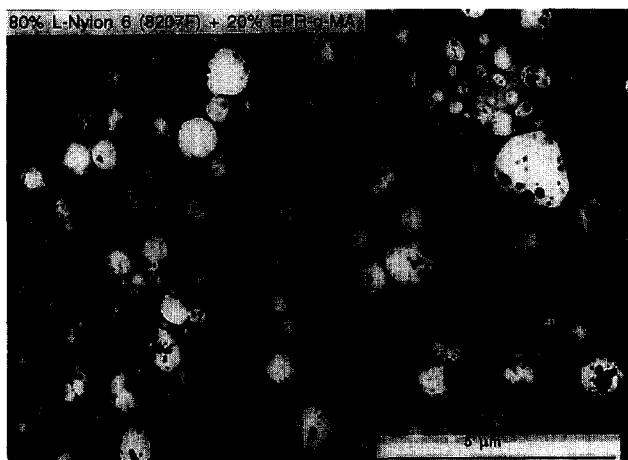


Figure 4 TEM photomicrograph of a blend of L-Nylon 6 with EPR-g-MA; PTA stained

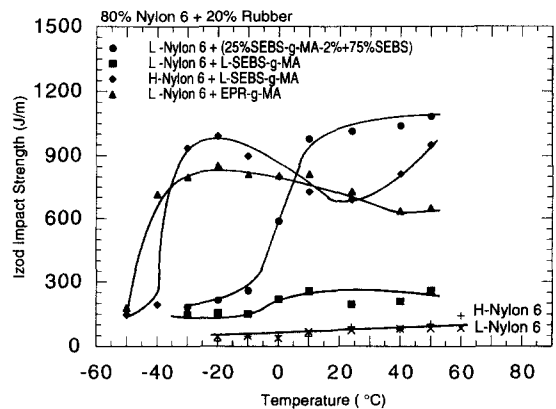


Figure 5 Notched Izod impact strength as a function of temperature for the various blends and neat nylon 6 materials

Table 3 Parameters characterizing the blend morphology and the fractured specimens

80% nylon 6 + 20% rubber	Average particle diameter \bar{d}_w (μm)	Deformed zone size from TEM a (μm)	Whitened zone size (mm)		Apparent cavitation of rubber particles
			A	B	
L-Nylon 6 + (25% SEBS-g-MA-2% + 75% SEBS)	0.202	75	1.8	1.9	extensive
L-Nylon 6 + L-SEBS-g-MA	0.062	< 1	< 0.1	< 0.1	none
H-Nylon 6 + L-SEBS-g-MA	0.056	20	< 0.1	< 0.1	little
L-nylon 6 + EPR-g-MA	0.406	50	0.9	2.6	extensive

Table 4 Summary of fracture energy results^a

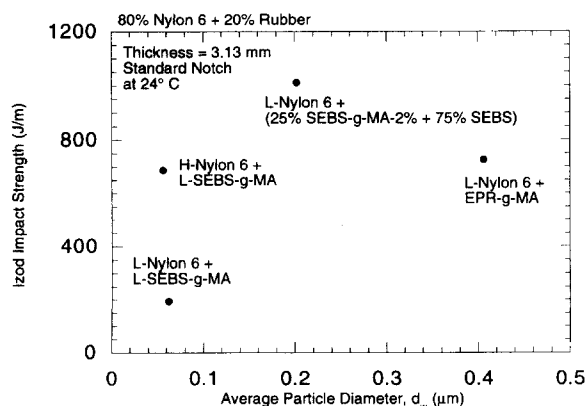
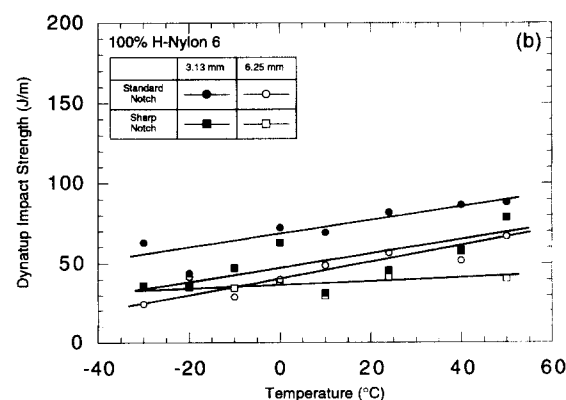
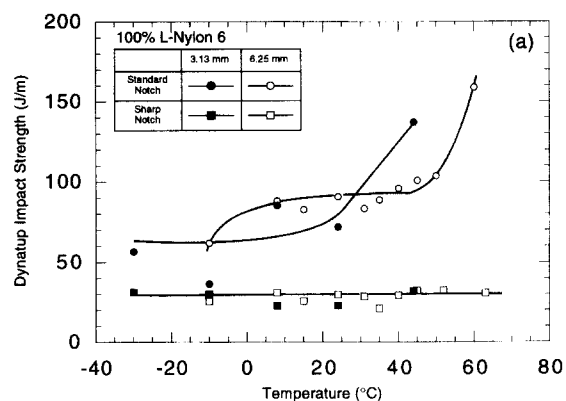
80% nylon 6 + 20% rubber	Izod impact (J m^{-1}) 3.18 mm Standard notch	Dynatup impact strength ^b (J m^{-1})				Vu-Khanh parameters G_i (kJ m^{-2}), T_a (10^6 kJ m^{-4})							
		3.18 mm		6.25 mm		3.18 mm		6.25 mm		3.18 mm		6.25 mm	
		Standard notch	Sharp notch	Standard notch	Sharp notch	G_i	T_a	G_i	T_a	G_i	T_a	G_i	T_a
						24°C	15°C (-10°C)	24°C	15°C (-10°C)	24°C	15°C (-10°C)	24°C	15°C (-10°C)
L-Nylon 6 + (25% SEBS-g-MA-2% + 75% SEBS)	1012 (0)	1644 (0)	1295 (0)	1443 (0)	1315 (0)	32.2	8.4	32.5	2.6	45.7	3.8	45.7	4.4
L-Nylon 6 + L-SEBS-g-MA	195 (0)	274 (-5)	205 (5)	180 (-5)	136 (5)	9.8	1.0	17.5	0.0	15.2	0.0	18.0	0.0
H-Nylon 6 + L-SEBS-g-MA	688 (-35)	1057 (-30)	1178 (-30)	515 (-30)	512 (-30)	20.1	2.7	49.9	1.3	27.9	0.6	29.2	0.4
L-Nylon 6 + EPR-g-MA	727 (-40)	879 (-20)	852 (-20)	694 (-20)	630 (-20)	43.6	2.7	31.7	1.2	34.7	1.2	34.6	1.0
L-Nylon 6	73	72	23	91	30	3.4	0.0	3.2	0.0	3.4	0.0	3.5	0.0
H-Nylon 6	88	82	45	57	42	—	—	—	—	3.3	0.0	—	—

^a Ductile–brittle transition temperature in parentheses^b Tested by Dynatup SN3PB at 24°C

of toughness with particle size is not expected¹⁴. For example, the blend of L-SEBS-g-MA with H-Nylon 6 shows a significantly higher impact strength than the corresponding blend with L-Nylon 6 in spite of the fact that both have almost the same average rubber particle size.

DYNATUP IMPACT STRENGTH AS A FUNCTION OF TEMPERATURE

Figure 7 shows the Dynatup impact strength for both neat nylon 6 materials as a function of temperature for thick (6.25 mm) and thin (3.13 mm) specimens with standard or

**Figure 6** Izod impact strength as a function of average rubber particle diameter**Figure 7** Dynatup impact strength as a function of temperature for (a) L-Nylon 6; (b) H-Nylon 6

sharp notches. Specimens with standard notches exhibit slightly higher impact strength for both specimen thicknesses; the notch sensitivity is greater for L-Nylon 6 than for H-Nylon 6 (see Figure 7b). Figure 8 shows a similar plot for the L-Nylon 6/25% SEBS-g-MA + 75% SEBS blend; in addition to the toughening this rubber phase provides, there is very little dependence of impact strength on specimen thickness or notch geometry. Figure 9 makes an analogous comparison of the Dynatup impact strength for blends of L-SEBS-g-MA rubber with L-Nylon 6 and with H-Nylon 6 as a function of temperature. The impact strength of the L-Nylon 6-based blend (Figure 9a) is much lower than that of the blend based on H-Nylon (Figure 9b). The low

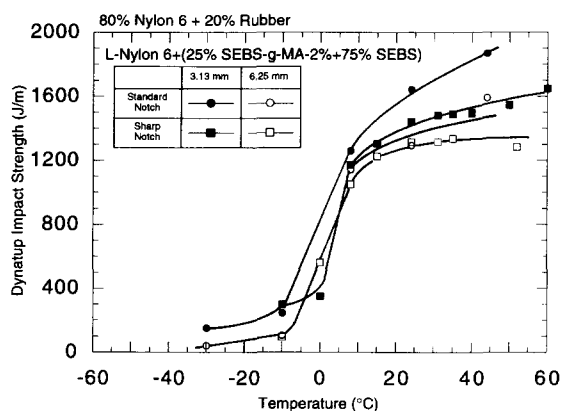


Figure 8 Dynatup impact strength as a function of temperature for the L-Nylon 6/75% SEBS-g-MA-2% + 25% SEBS blend for two sample thicknesses and notch geometries

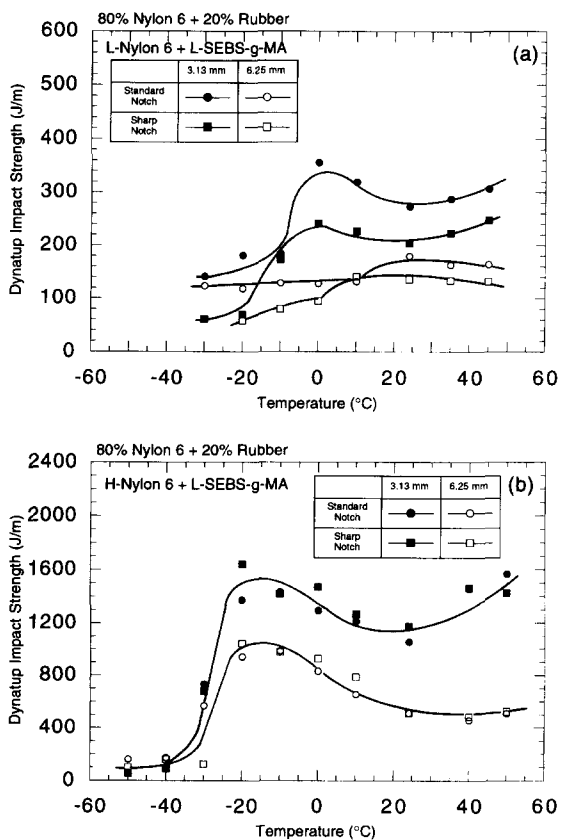


Figure 9 Dynatup impact strength as a function of temperature for (a) the L-Nylon 6/L-SEBS-g-MA blend and (b) the H-Nylon 6/L-SEBS-g-MA blend for two sample thicknesses and notch geometries

molecular weight nylon 6 blend has a stronger dependence on specimen geometry; both blends show some notch sensitivity. The H-Nylon 6/L-SEBS-g-MA blend exhibits a maximum in Dynatup impact strength at a temperature, -20°C , just above its ductile–brittle transition (Figure 9b). The L-Nylon 6/EPR-g-MA blend exhibits somewhat similar behaviour (see Figure 10) to the H-Nylon 6/L-SEBS-g-MA blend, i.e., high impact toughness just above the ductile–brittle transition temperature and little sensitivity to specimen geometry.

Table 4 summarizes the Dynatup impact strength values at room temperature. Generally, for both thicknesses, specimens with standard notches show higher impact strength than ones with sharp notches.

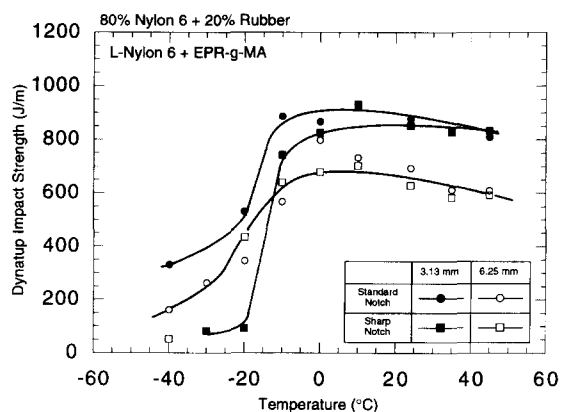


Figure 10 Dynatup impact strength as a function of temperature for the L-Nylon 6/EPR-g-MA blend for two sample thicknesses and notch geometries

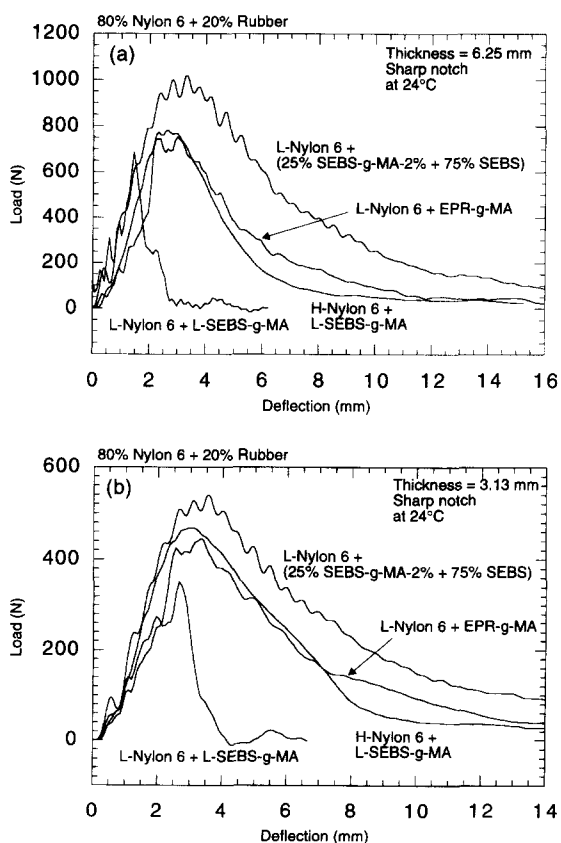


Figure 11 Dynatup load–deflection curves for various blends at 24°C for (a) thick and (b) thin specimens with sharp notches

IMPACT LOAD CURVE ANALYSIS

The impact load–deflection curves obtained during Dynatup SN3PB testing were signal-conditioned using a digital low-pass filter⁵¹. Sample curves measured at room temperature are shown in *Figure 11a* for thick (6.25 mm) specimens with sharp notches, and in *Figure 11b* for thin (3.13 mm) specimens with sharp notches. Of the four blends under consideration, L-Nylon 6/(25% SEBS-g-MA-2% + 75% SEBS), which has the highest Izod and Dynatup impact toughness at room temperature, shows the highest impact load and deflection during fracture for both thicknesses. Differences in the impact load–deflection curves for the various blends are more exaggerated for thick specimens than for thin specimens.

Figure 12 shows impact load–deflection curves measured at three different temperatures for two blend systems. For the L-Nylon 6/(25% SEBS-g-MA-2%/75% SEBS) blend, the load level increases continuously as the temperature is raised over this range and is consistent with the corresponding increase in impact strength noted for this blend over this temperature range (see *Figures 5, and 8*). The load–deflection curves for the H-Nylon 6/L-SEBS-g-MA blend show the highest load at the lowest temperature, -10°C . However, this is consistent with the maximum in impact strength in the region of -10°C seen in *Figures 5, and 9b*. Likewise, the lower loads seen at 24°C are consistent with the minimum in impact strength seen at about this temperature in *Figures 5, and 9* for this blend. The subsequent rise in impact strength at higher temperature is not so readily explained by the load–deflection curves at 50°C which are not substantially different from those seen at 24°C .

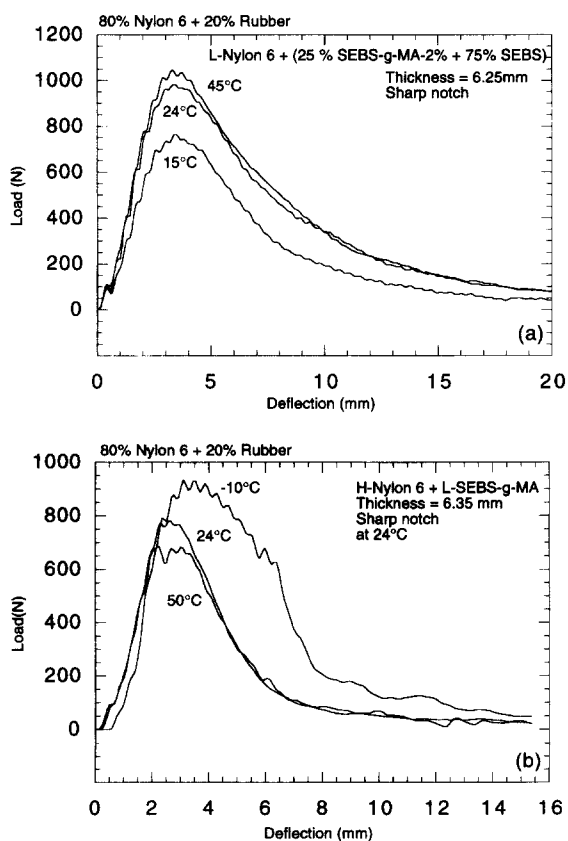


Figure 12 Dynatup load–deflection curves for various temperatures for thick specimens with sharp notches for (a) the L-Nylon 6/75% SEBS-g-MA-2% + 25% SEBS blend; (b) the H-Nylon 6/L-SEBS-g-MA blend

VU-KHANH FRACTURE PARAMETERS

The fracture toughness parameters defined by Vu-Khanh³⁶ were obtained by the procedures reported in previous papers⁵¹. In this representation, the fracture energy per unit of ligament area, U/A , is a linear function of the ligament area A which can be described by the two parameters defined by the relationship

$$\frac{U}{A} = G_i + \frac{1}{2}T_a A \quad (2)$$

The quantity G_i has been termed the fracture energy at initiation, while T_a has been interpreted as the tearing modulus.

Figure 13 shows the fracture energy per unit area for the materials in *Table 2* as a function of ligament area obtained at room temperature using thick (*Figure 13a*) and thin (*Figure 13b*) specimens with sharp notches. The tearing modulus, T_a , of neat nylon 6 and the L-Nylon 6/L-SEBS-g-MA blend is zero when thick specimens are used, indicative of the brittle nature of these materials; however, this blend has a small but finite tearing modulus when thin specimens are used. All of the rubber-toughened blends have significantly higher values of the fracture energy at initiation, G_i , than either neat nylon 6, for both specimen geometries. *Figure 14* shows the Vu-Khanh plots for two blends as a function of temperature (similarly to *Figure 13*), using thick specimens with sharp notches. For the L-Nylon 6/(SEBS-g-MA-2%/SEBS) blend (*Figure 14a*), the tearing modulus increases with temperature while fracture energy at initiation increases slightly. The results for the H-Nylon 6/L-SEBS-g-MA blend (*Figure 14b*) show that the fracture energy at initiation is significantly higher at -10°C than at other temperatures. The values of both G_i and T_a are about the same at 24°C and at 50°C . The fracture energy at initiation, G_i , and tearing modulus, T_a , obtained for each

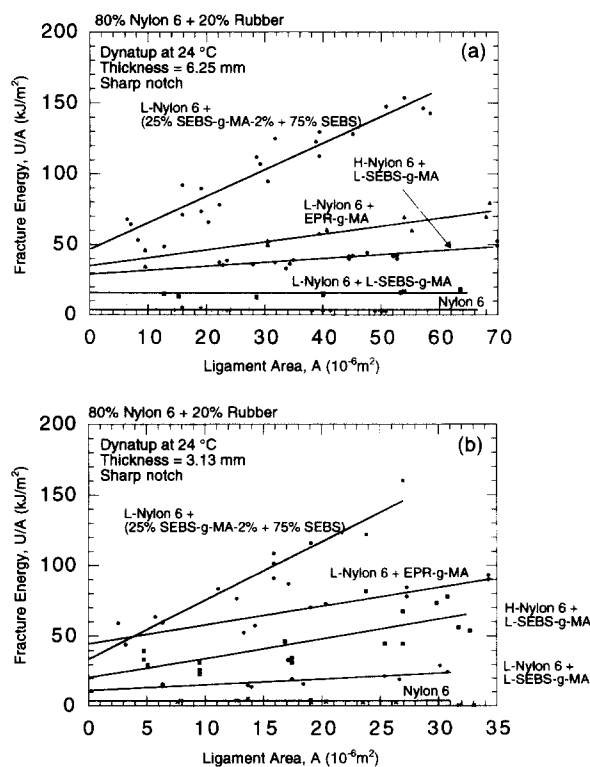


Figure 13 Fracture energy as a function of ligament area for (a) thick and (b) thin specimens with sharp notches for various blends at 24°C

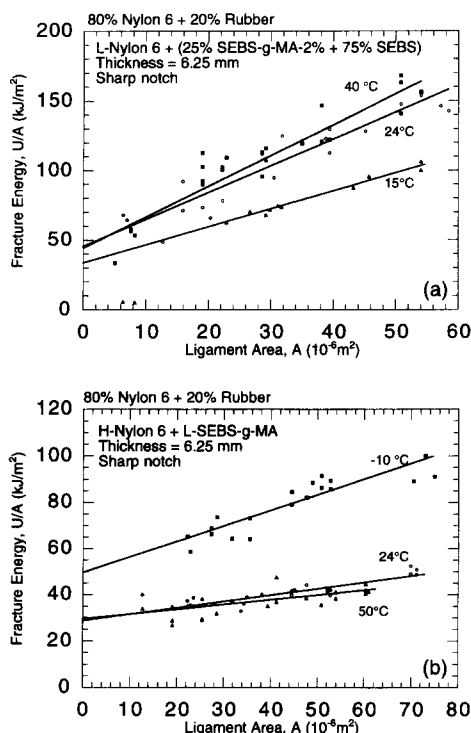


Figure 14 Fracture energy as a function of ligament area for thick specimens with sharp notches for (a) the L-Nylon 6/75% SEBS-g-MA-2% + 25% SEBS blend and (b) the H-Nylon 6/L-SEBS-g-MA blend at various temperatures

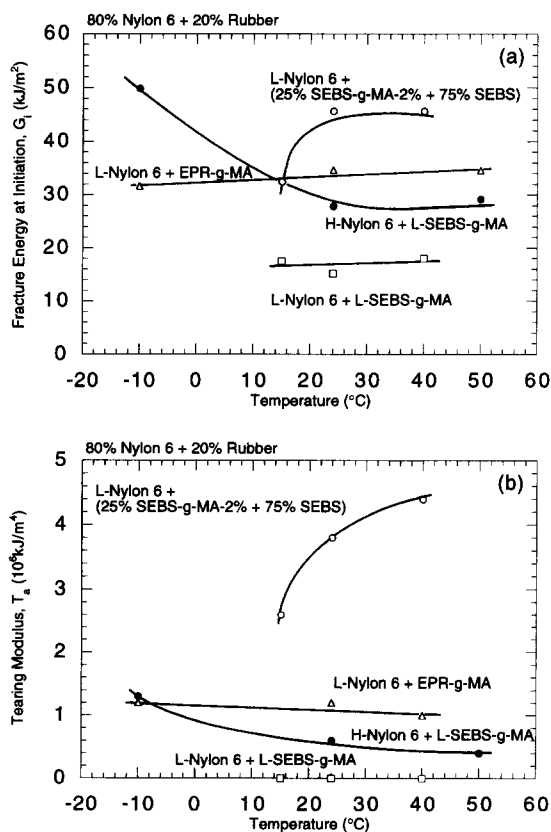


Figure 15 Fracture energy at initiation (a) and tearing modulus (b) as a function of temperature for various blends

blend in Table 2 at several temperatures are summarized in Table 4 and in Figure 15. The effects of temperature on these parameters are substantially different between these blends, and at this point it is not apparent how to interpret in detail these different trends for the H-Nylon 6/L-SEBS-g-MA blend. The fracture energy at initiation is high at low temperatures and decreases with increasing temperature. For the other blends, this quantity increases slightly with increasing temperature. The tearing modulus for the L-Nylon 6/(25% SEBS-g-MA-2% + 75% SEBS) blend is quite high and increases with temperature (Figure 15b). The tearing modulus for the L-Nylon 6/L-SEBS-g-MA blend is essentially zero at all temperatures. The remaining two blends have intermediate values of the tearing modulus, and the values decrease slightly with increasing temperature. The higher toughness of L-Nylon 6/(25% SEBS-g-MA-2% + 75% SEBS) at high temperatures is based on the increase in the tearing modulus, whereas the higher toughness of this material at -10°C is based on its high fracture energy at initiation at this temperature. These results show the benefit of such a detailed analysis, in comparison to Izod or Charpy type testing, by differentiating the extent that changes in energy to produce a complete fracture stem from changes in the fracture energy at initiation, G_i , and/or the changes in the tearing modulus, T_a . More extensive investigations are required to understand fully how the properties and structure of the rubber phase, rubber particle diameter, and polyamide molecular weight influence these parameters.

OBSERVATION OF THE REGION AROUND THE ARRESTED CRACK

In order to understand the deformation processes that occur in nylon 6 blends toughened by these various types of rubber, cracks formed during high speed testing of 6.25 mm thick specimens with sharp notches were arrested and the surrounding region was examined by TEM using the techniques described earlier⁵¹.

Figure 16 shows the region near the crack path for the L-Nylon 6/L-SEBS-g-MA blend stained by RuO₄. The photomicrograph reveals that this blend does not show any cavitation of the rubber particles or shear yield zone under the high speed fracture process. This observation is consistent with the low Izod and Dynatup impact strengths of this blend. This blend also has a zero tearing modulus.

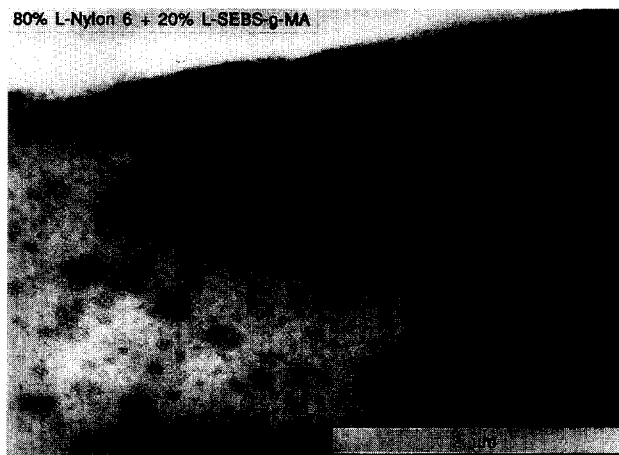


Figure 16 TEM photomicrograph showing the morphology of the deformed zone in the vicinity of the arrested crack for an L-Nylon 6/L-SEBS-g-MA blend

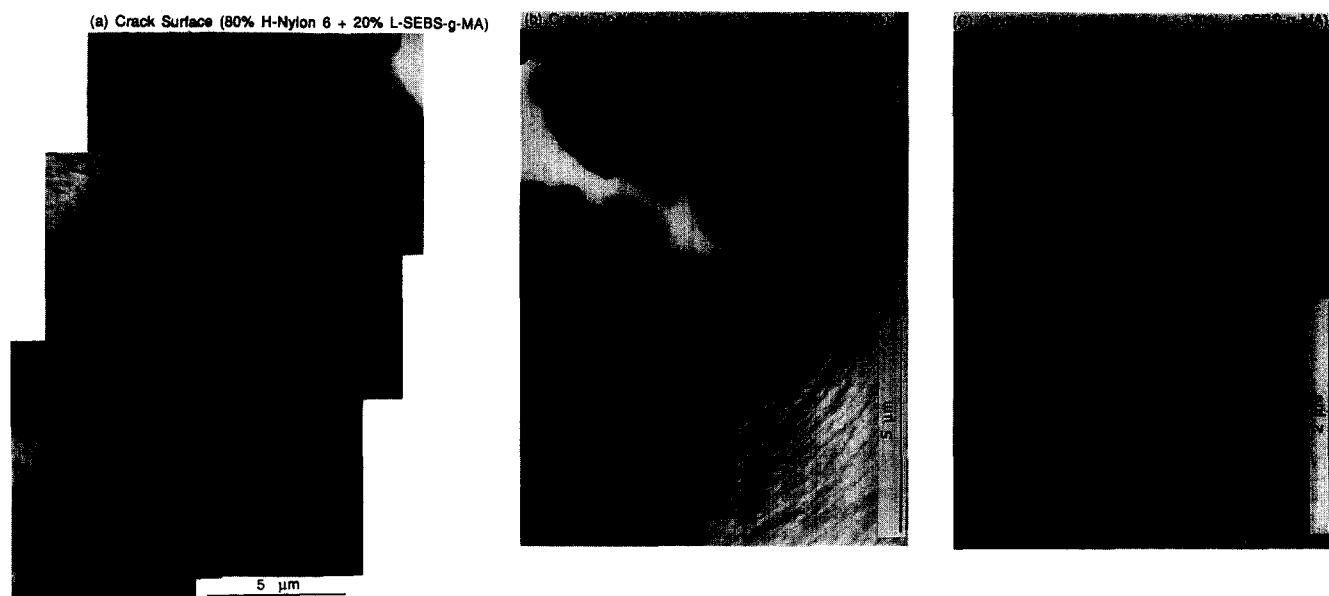


Figure 17 TEM photomicrographs showing the deformed zone morphology (a) along the crack surface, (b) near the crack tip and (c) ahead of the crack tip for an H-Nylon 6/L-SEBS-g-MA blend

Figure 17 is a composite of several photomicrographs depicting the region near and well forward of the arrested crack tip for the tough H-Nylon 6/L-SEBS-g-MA blend stained by RuO₄. Figure 17a reveals three roughly separate regions: a zone of extensive shear yielding, a zone of shear yielding, and a zone where rubber particles cavitate. Figure 17b shows branching and blunting of the crack tip in this blend. These observations are very similar to those for various nylon 6 blends with SEBS-g-MA-2% SEBS mixtures, as reported previously⁵¹. It is interesting to note that rubber particles of very similar size formed from L-SEBS-g-MA readily cavitate when the matrix is H-nylon 6 but do not cavitate when the matrix is L-Nylon 6; the mechanistic reason for this difference is not clear at this time. Both L-Nylon 6 and H-Nylon 6 have nearly the same toughness as measured by various methods (see Table 4). The molecular weight of the nylon 6 matrix does, of course, influence its viscoelastic, yield, etc. characteristics, but the connection of such properties to these dramatic differences in fracture behaviour is not easy to make.

Figure 18 shows the region near the crack path for the L-Nylon 6/EPR-g-MA blend stained by PTA. This blend shows massive cavitation around the crack path. Holes arising from rubber particle cavitation are observed even very near the crack surface; blends based on the SEBS type of rubber show massive yielding near the crack surface in which the holes formed by rubber particle cavitation have collapsed. This difference may be related to the size of rubber particles or the holes formed by cavitation. The average size of the rubber particles and the holes formed in them by cavitation are much larger for the blends based on EPR-g-MA than those based on the SEBS type of rubber (Table 3, Figure 17c and Figure 19). Shear yielding of the matrix, which occurs after the rubber particles cavitate, may not be able to collapse these holes.

Using composites of several TEM microphotographs, the size of the deformed zone, a , as shown schematically in Figure 19a, was determined. Values of the thickness, a , for the blends examined here varied from 0 to 75 μm . This is much smaller than the size of the whitened zone defined in Figure 9b, which ranges from 0.1 mm to 1.8 mm; however,



Figure 18 TEM photomicrograph showing the morphology of the deformed zone in the vicinity of the arrested crack for the L-Nylon 6/EPR-g-MA blend

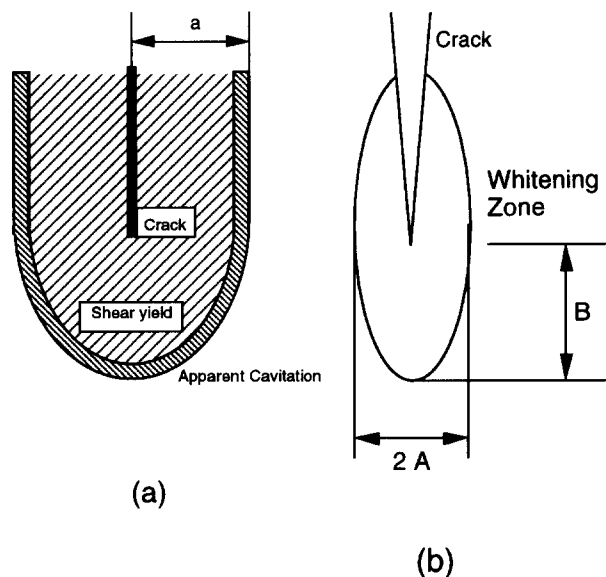


Figure 19 Schematic showing (a) the deformed zone as observed by TEM and (b) the whitened zone as observed by eye in the vicinity of the arrested crack tip

there is a definite correlation between the size of the visually observed whitened zone and the size of the deformed zone seen in TEM photomicrographs (see Table 3). Figure 20a shows room-temperature Dynatup impact strength values obtained for thick specimens with sharp notches as a function of the deformed zone size for the materials studied here, along with previously reported results. The impact strength of blends based on various rubber types increases in proportion to the increase in the deformed zone size, a . This suggests that the main mechanism of energy absorption is plastic deformation of the nylon 6 matrix induced by rubber particle cavitation and that energy absorption per unit volume is essentially not influenced by the type of rubber used; however, the type of rubber, rubber particle size, and concentration of rubber acts to change the size of the deformed zone size.

The Vu-Khanh fracture parameters, G_i and T_a , strongly correlate with the size of the deformed zone, a , as shown in Figure 20b and c⁵¹. The so-called fracture energy at initiation, G_i , for the various blends forms a unique linear relationship independent of the rubber type. Figure 20c shows that the tearing modulus is zero until the deformed zone is larger than a certain critical value; after this, there is a linear relationship between these parameters. Since both G_i and T_a appear to be related to the size of the deformed zone, it is clear that these two parameters are not fully independent of each other, at least for the blends shown, as shown by the strong correlation between G_i and T_a visible in Figure 21. It should be pointed out that addition of rubber in a suboptimal manner does increase G_i , while T_a remains zero; however, beyond a certain point further improvements in G_i seem to lead to increased values of T_a as well. It is not yet clear how effectively the two parameters can be varied independently by formulation.

From these results presented here, it is clear that the energy absorption for these rubber-toughened blends stems mainly from plastic deformation of the matrix which is induced by rubber cavitation. Differences in rubber particle size and type of rubber change the threshold stress at which the cavitation of rubber particles begins.

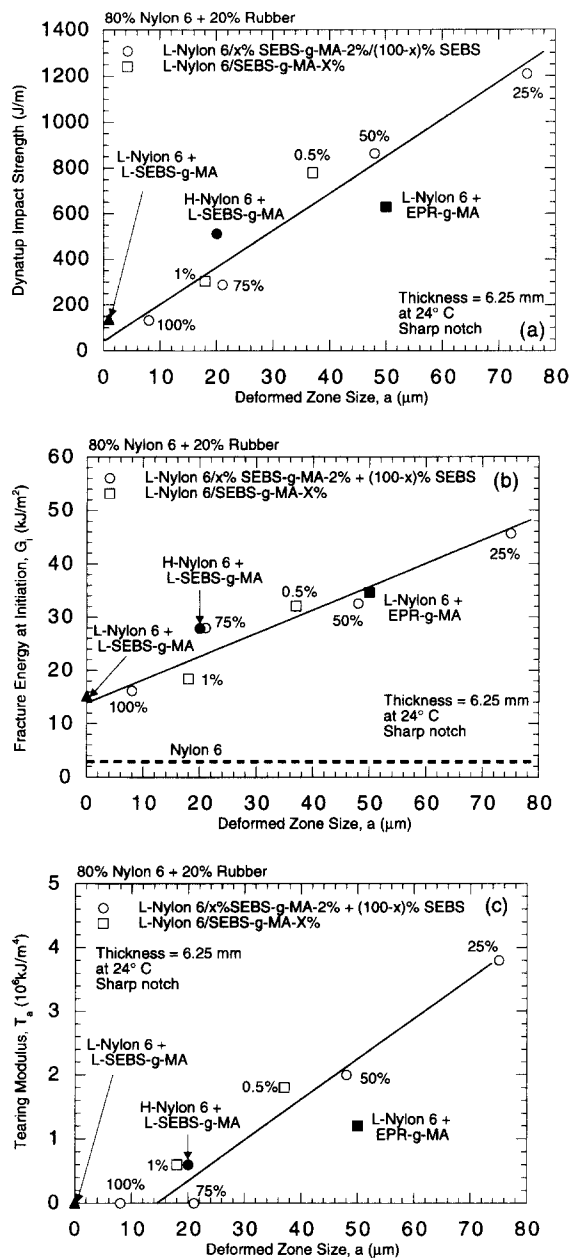


Figure 20 Dynatup impact strength (a), fracture energy at initiation (b) and tearing modulus (c) as a function of deformed zone size, a , for thick specimens with sharp notches at 24°C

SUMMARY AND CONCLUSIONS

As described in previous reports, rubber particle size is one of the most important factors determining the toughness of rubber-modified nylon 6 blends; however, the chemical structure of the rubber and the properties of the matrix have considerable influence on the toughness of the blends. This study has shown that a linear relationship of toughness parameters, Dynatup impact strength, fracture energy at initiation and tearing modulus, versus the deformed zone size, exists for all the blends studied here regardless of rubber type or matrix molecular weight. This suggests that the energy absorption for these rubber-toughened blends stems mainly from plastic deformation of the matrix, as induced by rubber cavitation. It is interesting to note that rubber particles of very similar size formed from L-SEBS-g-MA (low system content) readily cavitate when the matrix is H-Nylon 6 (high molecular weight) but do not cavitate when

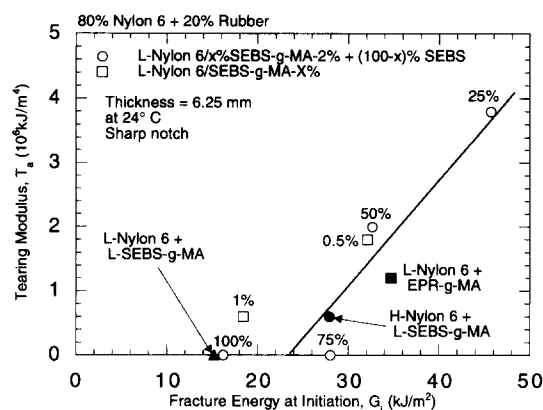


Figure 21 Fracture energy at initiation, G_i , as a function of tearing modulus, T_a , for thick specimens with sharp notches at 24°C

the matrix is L-Nylon 6 (low molecular weight), even though L-Nylon 6 and H-Nylon 6 have nearly the same toughness as measured by various methods. The molecular weight of the nylon 6 matrix does, of course, influence its viscoelastic, yield, etc. characteristics, but the connection of such properties to these dramatic differences in fracture behaviour is not easy to make at this point. Further work is needed to show how the properties of the matrix influence the cavitation of rubber particles.

ACKNOWLEDGEMENTS

This research was supported by the US Army Research Office and Mitsubishi Gas Chemical Co. The authors express their appreciation to Allied-Signal Inc., Exxon Chemical Co. and Shell Development Co. for providing the various materials used in this research.

REFERENCES

- Lawson, D.F., Hergenrother, W.L. and Matlock, M.G., *J. Appl. Poly. Sci.*, 1990, **39**, 2331.
- Gilmore, D. W. and Modic, M. J., *Plastics Eng.*, 1989 (April), 29.
- Wu, S., *J. Appl. Poly. Sci.*, 1988, **35**, 549.
- Borggreve, R.J.M., Gaymans, R.J. and Eichenwald, H.M., *Polymer*, 1989, **30**, 78.
- Hobbs, S.Y., Bopp, R.C. and Watkins, V.H., *Polym. Eng. Sci.*, 1983, **23**, 380.
- Borggreve, R.J.M., Gaymans, R.J., Schuijjer, H. and Ingen Housz, J.F., *Polymer*, 1987, **28**, 1489.
- Epstein, B. N., US Patent No. 4 174 358 (to DuPont). 1989.
- Wu, S., *Polym. Eng. Sci.*, 1987, **27**, 335.
- Borggreve, R.J.M. and Gaymans, R.J., *Polymer*, 1989, **30**, 63.
- Borggreve, R.J.M., Gaymans, R.J. and Schuijjer, J., *Polymer*, 1989, **30**, 71.
- Oshinski, A.J., Keskkula, H. and Paul, D.R., *Polymer*, 1992, **33**, 268.
- Oshinski, A.J., Keskkula, H. and Paul, D.R., *Polymer*, 1992, **33**, 284.
- Oshinski, A.J., Keskkula, H. and Paul, D.R., *Polymer*, 1996, **37**, 4891.
- Oshinski, A.J., Keskkula, H. and Paul, D.R., *Polymer*, 1996, **37**, 4909.
- Oshinski, A.J., Keskkula, H. and Paul, D.R., *Polymer*, 1996, **37**, 4919.
- Fayt, R., Jerome, R. and Teyssie, R., *ACS Symp. Ser.*, 1989, **395**, 38.
- Lambla, M., Yu, R.X. and Lorek, S., *ACS Symp. Ser.*, 1989, **385**, 67.
- Cimmino, S., Coppola, F., D'Orazio, L., Greco, R., Maglio, G., Malianconico, M., Mancerella, C., Martuscelli, E. and Ragosta, G., *Polymer*, 1986, **27**, 1874.
- Bucknall, C. B., *Toughened Plastics*. Applied Science, London, 1977.
- Boyer, R. F. and Keskkula, H., in *Encyclopedia of Science and Technology*, Vol. 13, ed. N. Bikales. John Wiley, New York, 1970, p. 375.
- Turley, S.G. and Keskkula, H., *Polymer*, 1980, **21**, 466.
- Donald, A.M. and Kramer, E.J., *Polymer*, 1985, **26**, 1855.
- Keskkula, H., *Adv. Chem. Ser.* **222** (ed. C. K. Riew). American Chemical Society, Washington, DC, 1989, p. 289.
- Wu, S., *J. Appl. Poly. Sci.*, 1988, **35**, 549.
- Bucknall, C.B., Heather, P.S. and Lazzeri, A., *J. Mater. Sci.*, 1989, **16**, 2255.
- Bucknall, C.B., Karpodinis, A. and Zhang, X.C., *J. Mater. Sci.*, 1994, **29**, 3377.
- Partidge, I., Sanz, C. and Bickerstaff, K., in *Proceedings of the Fifth Annual Meeting of the Polymer Processing Society*, Tokyo, Japan, 1989, p. 218.
- Bernstein, H. L., Fracture toughness of polycarbonate as characterized by the J -integral, in *Elastic-Plastic Test Methods: The User's Experience*, Vol. 2, ASTM STP 1114, ed. J. A. Joyce. ASTM, Philadelphia, 1991, p. 306.
- Chung, W. N. and Williams, J. G., Determination of J_{1c} for polymers using the single specimen method, in *Elastic-Plastic Test Methods: The User's Experience*, Vol. 2, ASTM STP 1114, ed. J. A. Joyce. ASTM, Philadelphia, 1991, p. 320.
- Crouch, B.A. and Huang, D.D., *J. Mater. Sci.*, 1994, **29**, 861.
- Duffy, J. and Shih, C. F., in *Advances in Fracture Research. Proceedings of the 7th International Conference on Fracture (ICF7)*. Pergamon Press, 1989, p. 633.
- Hashemi, S. and Williams, J.G., *J. Mater. Sci.*, 1991, **26**, 621.
- Huang, D. D., The application of the multispecimen J -integral technique to toughened polymers, in *Elastic-Plastic Test Methods: The User's Experience*, Vol. 2, ASTM STP 1114, ed. J. A. Joyce. ASTM, Philadelphia, 1991, p. 290.
- Mai, Y.-W. and Powell, P., *J. Polym. Sci.: Part B: Polym. Phys.*, 1991, **29**, 785.
- Takemori, M. T. and Narisawa, I., in *Advances in Fracture Research. Proceedings of the 7th International Conference on Fracture (ICF7)*. Pergamon Press, 1989, p. 2733.
- Vu-Khanh, T., *Polymer*, 1979, **1988**, 29.
- Wu, J. and Mai, Y.-W., *J. Mater. Sci.*, 1993, **28**, 6167.
- Vu-Khanh, T. and De Charentenay, F.X., *Polym. Eng. Sci.*, 1985, **25**, 841.
- Paton, C.A. and Hashemi, S., *J. Mater. Sci.*, 1992, **27**, 2279.
- Zhou, Z., Landes, J.D. and Huang, D.D., *Polym. Eng. Sci.*, 1994, **34**, 128.
- Huang, D.D. and Williams, J.G., *J. Mater. Sci.*, 1987, **22**, 2503.
- Huang, D.D., *Soc. Plast Eng., ANTEC*, 1991, **49**, 582.
- Seidler, S. and Grellmann, W., *J. Mater. Sci.*, 1993, **28**, 4078.
- American Society for Testing and Materials, E-399: Standard test method for plane-strain fracture toughness of metallic materials, in *Annual Book of ASTM Standards*. ASTM, Philadelphia, 1990.
- Williams, J. G., *Fracture Mechanics of Polymers*. Ellis Horwood, Chichester, 1984.
- American Society for Testing and Materials, E-813: Standard test method for J_{1c} , a measure of fracture toughness, in *Annual Book of ASTM Standards*. ASTM, Philadelphia, 1989.
- Mai, Y.-W., *Polym. Comm.*, 1989, **30**, 330.
- Mai, Y.-W. and Cotterell, B., *Int. J. Fract.*, 1986, **32**, 105.
- Mai, Y.-W., Cotterell, B., Horlck, R. and Vigna, G., *Polym. Eng. Sci.*, 1987, **27**, 804.
- Hodgkinson, J.M. and Williams, J.G., *Mater. Sci.*, 1981, **16**, 50.
- Kayano, Y., Keskkula, H. and Paul, D.R., *Polymer*, 1985, **1997**, 38.
- Chung, I., Throckmorton, E. and Chundury, D., *Soc. Plast. Eng., ANTEC*, 1979, **37**, 681.
- Pai, Chih-Chiang Jeng, Grossman, Ru-Jong, Steven, J. and Huang, Jan-Chan, *Adv. Polym. Tech.*, 1989, **2**, 157.
- Kayano, Y., Keskkula, H. and Paul, D. R., *Polymer*, 1997, **38**, 1885.